Bull. Chem. Soc. Jpn., 75, 1371–1379 (2002)

Non-Linearity and Non-Additivity of Substituent Effects in Solvolysis of 1,1-Diphenylethyl *p*-Nitrobenzoates

Md. Khabir Uddin, Mizue Fujio,* Hyun-Joong Kim, Zvi Rappoport, and Yuho Tsuno

Institute for Fundamental Research of Organic Chemistry, Kyushu University, Higashi-ku, Fukuoka, 812-8581

(Received December 25, 2001)

The solvolysis rates of 1,1-diarylethyl *p*-nitrobenzoates and chlorides Y-Ar(X-Ar)CMe-L$_G$ (L$_G$ = OPNB, Cl) have been determined conductimetrically at 25 °C in 80% (v/v) aqueous acetone. A linear Yukawa–Tsuno (Y–T) correlation was found for the symmetrical subseries (X = Y), showing a precise additivity relationship for the whole substituent range with $\rho_{\mathrm{sym}} = -3.78$ and $r_{\mathrm{sym}} = 0.77$. The unsymmetrical subsets (X ≠ Y) gave statistically less reliable Y–T correlations, the apparent ρ value decreasing significantly when the fixed substituent Y becomes more electron-donating, which is in line with expectations from the Reactivity-Selectivity Relationship. In the whole dispersion pattern, both strong *p*-π-donor and electron-withdrawing substituents in any fixed-Y subsets exhibit significant rate-enhancement deviations from the points of X = Y on the reference ρ_{sym} line, which suggests an anti-Hammond shift of the transition state. However, there was a precise *Extended Brønsted Linear Relationship* between the p$K_{\mathrm{R^+}}$ values for the hydration of 1,1-diarylethylenes and the rates of solvolysis of the *p*-nitrobenzoates with a slope of unity ($\alpha = 1.03$). This is direct, convincing evidence that there is no significant shift of the transition-state coordinate over the whole range of substituent change.

The Yukawa–Tsuno (Y–T) equation 1[1] has been successfully applied to the *Structure–Reactivity Relationship* of a variety of benzylic carbocation systems[2,3] where direct π-delocalization of the cationic charge into the ring is possible.

$$\log(k/k_0) = \rho(\sigma^0 + r\Delta\bar{\sigma}_{\mathrm{R}}^{+}) \tag{1}$$

Here σ^{o} is the normal substituent constant and $\Delta\bar{\sigma}_{\mathrm{R}}^{+}$ is the resonance substituent constant measuring the donor capability of π-electron donating substituents.[1b] The parameter r is a measure of the resonance demand of the given reaction, i.e., the degree of resonance interaction between the aryl group and the reaction site in the transition state.[1–3] Thus the Y–T equation allows one to define the intrinsic $\bar{\sigma}$ scale inherent in the system, and to derive the appropriate ρ_{X} as the reference capable of detecting non-linearity and non-additivity of substituent effects.

Substituent effects on rates[4a] and equilibria[5] of the heterolytic formation of benzhydryl and trityl cations[6] were analyzed in terms of a selectivity relationship,[7] or of a coordinate-shift of the transition state.[7,8a] However, the non-linearity of substituent effects invalidated the conclusion of such solvolysis. Our argument against this conclusion for more extensive data sets[4c] was presented in our review.[3]

The earlier data for the solvolysis of benzhydryl chlorides[4a,b] indicated that the kinetic effects of multiple substituent change on different aromatic rings were not additive. Nishida[4a] related the reaction constant $(\rho_{\mathrm{X}})_{\mathrm{Y}}$, or simply ρ_{Y}, for the effect of substituents X in the fixed Y subset to the $\bar{\sigma}_{\mathrm{Y}}$ of Y by Eq. 2.

$$(\rho_{\mathrm{X}})_{\mathrm{Y}} = (\rho_{\mathrm{X}})_{\mathrm{H}} + q\bar{\sigma}_{\mathrm{Y}} \tag{2}$$

Here $(\rho_{\mathrm{X}})_{\mathrm{H}}$, or simply ρ_{H}, is the ρ_{X} value for the monosubstituted (Y = H) subset, and q is the coefficient for the Y-dependency of ρ_{X} or $(\rho_{\mathrm{X}})_{\mathrm{Y}}$. A general relationship to deal with multiple substituent effects (Eq. 3) was proposed.[5,7–9] It describes the non-additive effect in terms of different reaction constants for X and Y substituents, presented in the form of Eq. 3a:

$$\log(k_{\mathrm{XY}}/k_{\mathrm{HH}}) = \rho_{\mathrm{H}}(\bar{\sigma}_{\mathrm{X}} + \bar{\sigma}_{\mathrm{Y}}) + q\bar{\sigma}_{\mathrm{X}}q\bar{\sigma}_{\mathrm{Y}} \tag{3}$$

$$= \rho_{\mathrm{H}}\bar{\sigma}_{\mathrm{Y}} + (\rho_{\mathrm{H}} + q\bar{\sigma}_{\mathrm{Y}})\bar{\sigma}_{\mathrm{X}} \tag{3a}$$

In Eq. 3a the first term $\rho_{\mathrm{H}}\bar{\sigma}_{\mathrm{Y}}$ is a constant for a fixed-Y-subset, i.e., Eq. 3a is reduced to Eq. 2. The non-additivity is therefore taken into account by the last term in Eq. 3, which involves the coefficient q, described as the interaction constant.[7,8a,9] However, the analyses very often have shortcomings due to the significant non-linearity of substituent correlations for any fixed-Y subsets.

The non-linearity in the correlations for the fixed-Y-subsets has been dealt with by the More O'Ferrall equation 4,[10]

$$\log(k_{\mathrm{X}}/k_{\mathrm{H}})_{\mathrm{Y}} = (\rho_{\mathrm{o}})_{\mathrm{Y}}\bar{\sigma}_{\mathrm{X}} + (2m)_{\mathrm{Y}}(\bar{\sigma}_{\mathrm{X}})^2 \tag{4}$$

where $(\rho_{\mathrm{o}})_{\mathrm{Y}}$ is the tangential ρ of the fixed-Y-subset at X = H, and the coefficient $(2m)_{\mathrm{Y}}$ is a susceptibility parameter describing the degree of curvature of correlations of a given Y-subset.

The selectivity parameter ρ for a reaction series shows a sensitive change when the reactivities (or the stabilities of transition states) of the parent substrates change. This behavior is often referred to as adherence to the Reactivity–Selectivity Relationship (RSR),[7,8b,11,12] in the sense that there is an inverse relationship between reactivity and selectivity insofar as both are

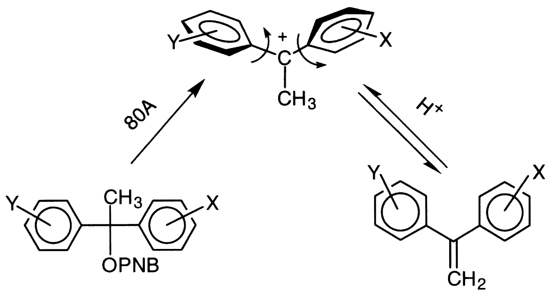

	variable	fixed
1	X	(Y = X)
2	X	(Y = H)
3	X	(Y = *p*-MeO)
4	X	(Y = *p*-Me)

Scheme 1.

related to shifts in the transition state position.[11] Dubois and co-workers carried out detailed analyses along similar lines for the bromination of disubstituted X-Ar(Y-Ar)C=CH_2 1,1-diarylethylenes, demonstrating that the $(\rho_X)_Y$ values significantly change linearly with σ^+ of Y.[13] Here again, any regression analysis displays severe non-linearity of substituent effect correlations of the respective fixed-Y subsets. Nevertheless, the authors concluded that the selectivities in the electrophilic additions are not directly related to the reactivities but to the position of the transition state.[13] They stated that bromination is a particularly attractive reaction for studying in detail the origin of Reactivity–Selectivity effects, since it is established that substituent effects arise both from changes in the stability of the cationic intermediate and from transition-state shifts,[7,8] in agreement with the RSR,[12,14] the Hammond postulate[12a] and Marcus effects.[15]

The progress of the reaction at this transition state is usually obtained from the Brønsted α coefficient (Eq. 5) or from other rate-equilibrium relationships[12]

$$\log (k_{XY}/k_{HH}) = \alpha(\Delta pK_{R^+}) \tag{5}$$

that compare substituent effects on kinetics and thermodynamics.

We have recently[16–18] investigated the non-linearity and non-additivity of the substituent effects on the solvolyses of the α-CF_3-diarylmethyl system. Whereas the symmetrical subseries (X = Y) gave an excellent linear Y–T correlation for the whole substituent range covering a reactivity change of 10^{12}, a precise simple additivity relationship exists only for the symmetrical subseries; it generally does not apply for any unsymmetrical subset (X ≠ Y). These nonlinear and non-additive substituent effects were ascribed to a substituent-induced conformation change of the two aromatic rings.

Similar effects should also be operative in the present α-Me-system, so that we should take into account here the non-additivity effect caused by both a substituent-induced conformational change and by coordinate-shifts of the transition state.

Accordingly, we had focused on exploring the scope of non-linearity and non-additivity behavior in the substituent effects on the solvolysis of the 1,1-diphenylethyl system, and carried out extensive studies on its solvolysis. The cation-forming solvolysis of this system is mechanistically connected to the reversible hydration[9] of 1,1-diphenylethylenes which proceeds via the same intermediate (Scheme 1). Both transition states should reflect any perturbation of the common intermediate, and the comparative studies will provide important information concerning the behavior of the transition states causing non-linearity and non-additivity.

In the first paper of this series, we have dealt with the substituent effects on the solvolysis of the parent, symmetrically disubstituted system **1** (X = Y) and monosubstituted **2** (Y = H) subsets, in this α,α-diaryl carbocation-forming reaction. We have attempted now to gain new insight into the causes of non-linearity and non-additivity behaviors through ordinary correlation analyses by using Eqs. 2–5.

Results

Solvolysis Rates. The rates of solvolysis of the *p*-nitrobenzoates, **1–4** (Scheme 1) and the corresponding chlorides were determined conductimetrically at 25 °C in 80% (v/v) aqueous acetone (80A) at initial concentrations of 10^{-5} – 10^{-4} mol dm^{-3} of the substrates. The reactions displayed accurate first-order kinetics over 2.5 half-lives and the reproducibility of the rate constants (k_{OPNB} and k_{Cl}) was estimated to be within ±1%. The slow solvolyzing derivatives were measured at 45 °C and the data were extrapolated to give the rates at 25 °C using the linear logarithmic rate relation between 25 °C and 45 °C; $\log k_{80A,25\,°C} = -0.906 + 1.059 \log k_{80A,45\,°C}$. The k_{OPNB} values were also measured in the faster solvolyzing solvent, 50% (v/v) aqueous acetone (50A) and converted to the rates in 80% (v/v) aqueous acetone at 25 °C by using $\log k_{80A,25\,°C} = -1.037 + 1.142 \log k_{50A,25\,°C}$. The k_{Cl} values were obtained for the highly deactivated derivatives and were converted to k_{OPNB} by the k_{OPNB}/k_{Cl} ratio of 1.03×10^{-5} derived from the average rate ratio for 1,1-diphenylethyl derivatives (**1**(H) and **1**(*p*-Cl)). Brown's rate data for **1**(H), **2**(*p*-CF_3), and **2**(3,5-$(CF_3)_2$) agreed with ours within the experimental uncertainty.[19] The rate of the *p*-MeO-substituted *p*-nitrobenzoate **2** (*p*-MeO) reported by Brown et al. was estimated from the rate of the benzoate using a ratio of 20.8, which is significantly different from our present solvolysis data.

The solvolysis rates and the activation parameters are summarized in Tables 1–4 together with Brown's data.

Correlation Analysis of Substituent Effects. The correlation analysis of substituent effects has been routinely carried out based on the Y–T equation 1, for the symmetrically disubstituted **1**, monosubstituted **2**, and some unsymmetrically disubstituted 1,1-diphenylethyl *p*-nitrobenzoates (**3** and **4**). The data are summarized in Table 5.

The substituent effects on the solvolysis of the symmetrical subseries **1** (X = Y) gave an excellent linear Y–T correlation (Table 5, entry 1 and Fig. 1) for the whole range of substituents with $\rho = -3.78$ and $r = 0.77$, with no noticeable deviation. In contrast, the correlation of the log $(k/k_0)_{OPNB}$ values for the whole set against $\bar{\sigma}_X + \bar{\sigma}_Y$ with the same r value of 0.77 as that for subseries **1** is poor, as demonstrated in Fig. 2. The simple additivity relationship (Eq. 6) against $\bar{\sigma}_X + \bar{\sigma}_Y$ instead of $2\bar{\sigma}_X$, gives a widely spread pattern for the whole set with partial correlations for different fixed-Y-subsets:

Table 1. Rates of Solvolysis of 1-Aryl-1-phenylethyl Chlorides (Cl) and *p*-Nitrobenzoates (OPNB) **2** in 80% Aqueous Acetone

X	$k_{\mathrm{Cl}}\times10^5/\mathrm{s}^{-1}$		$k_{\mathrm{OPNB}}\times10^5/\mathrm{s}^{-1}$		$\Delta H^{\ddagger}_{25\,°\mathrm{C}}$ [a]	$\Delta S^{\ddagger}_{25\,°\mathrm{C}}$ [a]
	45 °C	25 °C	45 °C	25 °C	kcal mol^{-1}	eu
p-MeO			692	63.0	22.0	0.6
p-MeS			90.5	7.00	23.5	1.4
p-MeO-*m*-Cl			32.3	2.61	23.1	−1.9
p-Me			15.87	1.28	23.1	−3.3
p-Et			12.94	1.00	23.5	−2.6
p-*t*-Bu			10.12	0.775	23.6	−2.7
p-MeS-*m*-Cl			5.66	0.354	25.5	2.0
m-Me			2.81	0.170	25.8	−1.7
H		8440	1.52	0.103	24.8	−2.8
				7.85×10^{-2} [b]		
p-Cl			0.415	2.48×10^{-2} [c]		
m-Cl				3.11×10^{-3} [d]		
m-CF_3				1.42×10^{-3} [d]		
p-CF_3				8.61×10^{-4} [d]		
				8.95×10^{-4} [b]		
3,5-Cl_2	132	14.25		1.47×10^{-4} [e]	20.4[f]	−7.7[f]
3,5-$(CF_3)_2$	26.1	2.79		2.88×10^{-5} [e]	22.4[f]	−4.6[f]
				4.31×10^{-5} [b]		

a) 1 cal = 4.184 J. b) Ref. 19. c) Estimated from $\log k_{80\mathrm{A},25°\mathrm{C}} = -0.906 + 1.059 \log k_{80\mathrm{A},45\,°\mathrm{C}}$. d) Estimated from $\log k_{80\mathrm{A},25\,°\mathrm{C}} = -1.037 + 1.142 \log k_{50\mathrm{A},25\,°\mathrm{C}}$. e) Estimated from chloride reactivities based on the average ratio of *p*-nitrobenzoate/chloride = 1.034×10^{-5} for **1**(X = H and X = *p*-Cl). f) Activation parameters are those for solvolysis of 1,1-diphenylethyl chlorides.

Table 2. Rates of Solvolysis of 1,1-Bis(substituted phenyl)ethyl Chlorides (Cl) and *p*-Nitrobenzoates (OPNB) **1** in 80% Aqueous Acetone

X	$k_{\mathrm{Cl}}\times10^5/\mathrm{s}^{-1}$		$k_{\mathrm{OPNB}}\times10^5/\mathrm{s}^{-1}$		$\Delta H^{\ddagger}_{25\,°\mathrm{C}}$ [a]	$\Delta S^{\ddagger}_{25\,°\mathrm{C}}$ [a]
	45 °C	25 °C	45 °C	25 °C	kcal mol^{-1}	eu
p-MeS			1167	111.3	21.6	0.3
p-Me			85.5	7.39	22.5	−2.0
p-MeS-*m*-Cl			9.81	0.808	23.0	−4.9
m-Me			4.53	0.294	25.2	0.7
p-Cl		625	9.50×10^{-2}	5.28×10^{-3} [b]		
p-Br		469		4.85×10^{-3} [c]		
m-Cl	64.4	6.29		6.50×10^{-5} [c]	21.3[d]	−6.2[d]
m-CF_3	12.45	1.187		1.23×10^{-5} [c]	21.6[d]	−8.8[d]

a) See footnote a in Table 1. b) See footnote c in Table 1. c) See footnote e in Table 1. d) See footnote f in Table 1.

Table 3. Rates of Solvolysis of Unsymmetrical 1,1-Diphenylethyl Chlorides (Cl) and *p*-Nitrobenzoates (OPNB), **3** (Y = *p*-MeO) and **4** (Y = *p*-Me), in 80% Aqueous Acetone

Y	X	$k_{\mathrm{Cl}}\times10^5/\mathrm{s}^{-1}$		$k_{\mathrm{OPNB}}\times10^5/\mathrm{s}^{-1}$		$\Delta H^{\ddagger}_{25\,°\mathrm{C}}$ [a]	$\Delta S^{\ddagger}_{25\,°\mathrm{C}}$ [a]
		45 °C	25 °C	45 °C	25 °C	kcal mol^{-1}	eu
p-MeO	*p*-Br			305	26.4	22.5	−2.0
	m-Cl			120.2	9.20	23.6	2.3
	m-CF_3				6.38		
	3,5-Cl_2			22.1	1.77	23.2	−2.4
	3,5-$(CF_3)_2$			12.46	0.85	24.7	1.0
p-Me	*m*-Cl			1.22	7.76×10^{-2} [b]		
	3,5-Cl_2		257		2.66×10^{-3} [c]		
	3,5-$(CF_3)_2$	690	76.7		7.93×10^{-4} [c]	20.1[d]	−5.3[d]

a) See footnote a in Table 1. b) See footnote c in Table 1. c) See footnote e in Table 1. d) See footnote f in Table 1.

Table 4. Rates of Solvolysis of 1,1-Diphenylethyl *p*-Nitrobenzoates (OPNB) in 50% Aqueous Acetone

X	Y	$k_{\mathrm{OPNB}} \times 10^5/\mathrm{s}^{-1}$		$\Delta H^{\ddagger}_{25\,°\mathrm{C}}$[a)]	$\Delta S^{\ddagger}_{25\,°\mathrm{C}}$[a)]
		45 °C	25 °C	kcal mol^{-1}	eu
H	*p*-Me	386	41.7	20.4	−5.6
	p-Et	374	34.8	21.8	−1.3
	p-*t*-Bu	280	26.6	21.6	−2.6
	m-Me	86.6	7.56	22.4	−2.2
	H	55.4	4.51	23.0	−1.2
	p-Cl	21.1	1.84	22.4	−5.1
	m-Cl	2.96	0.217	24.1	−3.8
	m-CF$_3$	1.608	0.109[b)]		
	p-CF$_3$	0.999	0.0657[b)]		
p-Cl	*p*-Cl	9.92	0.703	24.4	−0.4
m-Cl	*p*-Me	37.1	3.36	22.1	−5.0
	m-Me	4.70	0.340	24.2	−2.5

a) See footnote a in Table 1. b) Estimated from k_{OPNB} at 45 °C from $\log k_{50\mathrm{A},25\,°\mathrm{C}} = -0.839 + 1.069 \log k_{50\mathrm{A},45\,°\mathrm{C}}$.

Table 5. Correlation Analysis of Substituent Effects Using the Yukawa–Tsuno Equation 1

No.	Systems	Substituents (X) range	n[a)]	ρ	r	R	SD
1	**1** (Y = X)	*p*-MeS –*m*-CF$_3$	9	−3.78 ± 0.09	0.77 ± 0.04	0.9990	±0.12
2		*m*-correlation	4	−3.93 ± 0.05		0.9999	±0.04
3	**2** (Y = H)	whole range	14	−3.68 ± 0.08	0.88 ± 0.04	0.9988	±0.10
4	**1** + **2**	equivalent class[b)]	14	−3.83 ± 0.06	0.76 ± 0.03	0.9990	±0.09
5	**3** (Y = *p*-MeO)	whole range[c,d)]	8	−1.97 ± 0.12	(1.33 ± 0.17)[e)]	0.9978	±0.10
6		H – 3,5-(CF$_3$)$_2$	6	−1.91 ± 0.10		0.9967	±0.07
7	**4** (Y = *p*-Me)	whole range[d)]	6	−3.23 ± 0.18	(0.99 ± 0.15)[e)]	0.9985	±0.15
8	(Y = *m*-Cl)[f)]	*p*-MeO – *m*-Cl	10	−4.61 ± 0.08	0.93 ± 0.03	0.9995	±0.05
9	(Y = 3,5-Cl$_2$)[f)]	*p*-MeO – H	9	−4.78 ± 0.26	1.09 ± 0.09	0.9976	±0.11
10	(Y = 3,5-(CF$_3$)$_2$)[f)]	*p*-MeO – H	11	−5.04 ± 0.18	1.14 ± 0.06	0.9984	±0.09

a) Number of substituents involved. b) Equivalent class comprises all X in the subseries **1** (X = Y), and *p*-Et, *p*-*t*-Bu, *m*-Me, *p*-Cl, and *m*-Cl for **2** (Y = H). c) The rate $k_{(p\text{-MeO})_2}$ is estimated by Y–T Eq. for **1** (X = Y) subseries (entry 1). d) The rate $k_{(p\text{-MeO},p\text{-Me})}$ is estimated by Eq. 4 for **3** (Y = *p*-MeO) (Table 6, entry 4). e) The *r* value should be statistically indefinite. f) Unpublished.

$$\log (k/k_0)_{\mathrm{X,Y}} = \rho_{\mathrm{sym}}(\bar{\sigma}_{\mathrm{X}} + \bar{\sigma}_{\mathrm{Y}}) \tag{6}$$

While Eq. 6 holds precisely (with $\rho_{\mathrm{sym}} = -3.83$, $r_{\mathrm{sym}} = 0.76$) for the closely limited substrates (Table 5, entry 4) where the two aryl-substituents X and Y are essentially kinetically equivalent, there is a significant deviation from additivity when $\bar{\sigma}_{\mathrm{X}}$ is different from $\bar{\sigma}_{\mathrm{Y}}$ of the fixed-Y, thus indicating the importance of the $q\,\bar{\sigma}_{\mathrm{X}}\,\bar{\sigma}_{\mathrm{Y}}$ term in Eq. 3. In a typical case, the wide-range additivity correlation cannot include the plots of the monosubstituted subset **2**; both strong *p*-π-donor and electron-withdrawing substituents exhibit significant rate-enhancement deviations (Fig. 2). The resulting concave plot, whose two extremes are bent back upward from the reference line, appears to be typical of any subset with a variable X- and a fixed Y-substituent in the α,α-diaryl system.[3]

For the monosubstituted subset **2**, however, a nearly precise Y–T correlation is obtained with a slightly lower $(\rho_{\mathrm{X}})_{\mathrm{Y}}$ value of (−3.68) and a higher *r* (0.88) than **1** (Table 5, entry 3 and Fig. 3). For the **3** (Y = *p*-MeO) subset where $\log k_{\mathrm{X}}$ for X = *p*-MeO was estimated from the Y–T correlation for subseries **1** (Table 5, entry 1 and Fig. 1), a good Y–T correlation with a reduced $(\rho_{\mathrm{X}})_{\mathrm{Y}}$ value was obtained, though the *r* value might not be statistically very reliable (Table 5, entry 5). A similar correlation with a reduced $(\rho_{\mathrm{X}})_{\mathrm{Y}}$ was obtained also for **4** (Y = *p*-Me) (Table 5, entry 7). In contrast, each of those subsets of variable X with fixed strong electron-withdrawing Y (Y = *m*-Cl, 3,5-Cl$_2$, and 3,5-(CF$_3$)$_2$), correlates linearly by Eq. 1 with significantly higher $(\rho_{\mathrm{X}})_{\mathrm{Y}}$ and *r* values than **1** (Table 5, entries 8–10), when the regression analysis includes additional points from unpublished data.[20]

While the Y–T correlation may be sometimes statistically a little uncertain or nonlinear, evidently the apparent $(\rho_{\mathrm{X}})_{\mathrm{Y}}$ value for Y–T correlations of variable X-substituents changes significantly for a fixed Y-substituent. A qualitative trend of inverse linear change of $(\rho_{\mathrm{X}})_{\mathrm{Y}}$, which tends to be more negative as Y becomes more electron-withdrawing, is apparent (Table 5). These results suggest that different Y–T correlations (Eq. 3a) with different *r* values for Y- and X-substituted aryls are required for dealing with the non-additivity behavior in the present reaction.

All the fixed-Y subsets give significantly concave correlations, each of which contacts the tangential correlation line de-

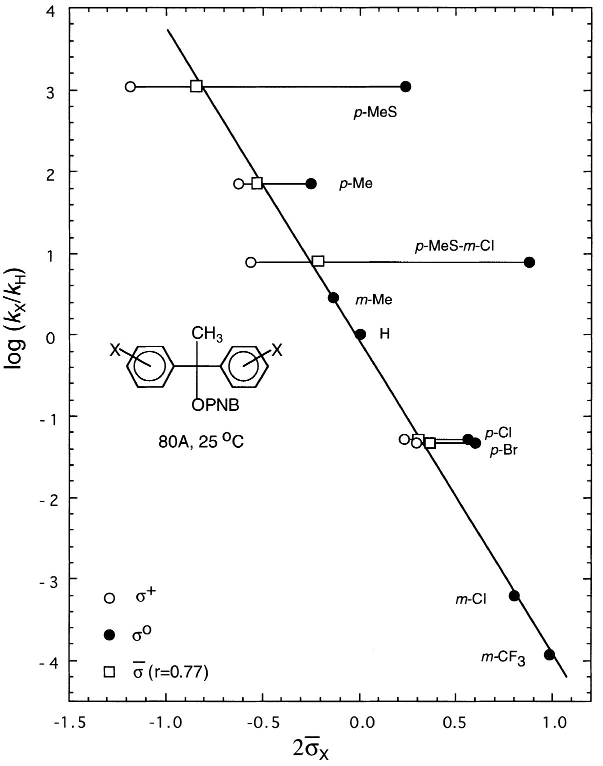

Fig. 1. Y–T plot for the solvolysis of symmetrically disubstituted 1,1-diphenylethyl *p*-nitrobenzoates **1**(X = Y) in 80% aqueous acetone at 25 °C: Closed circles for $2\sigma^o$, open circles for $2\sigma^+$, and open squares for $2\bar{\sigma}$, respectively.

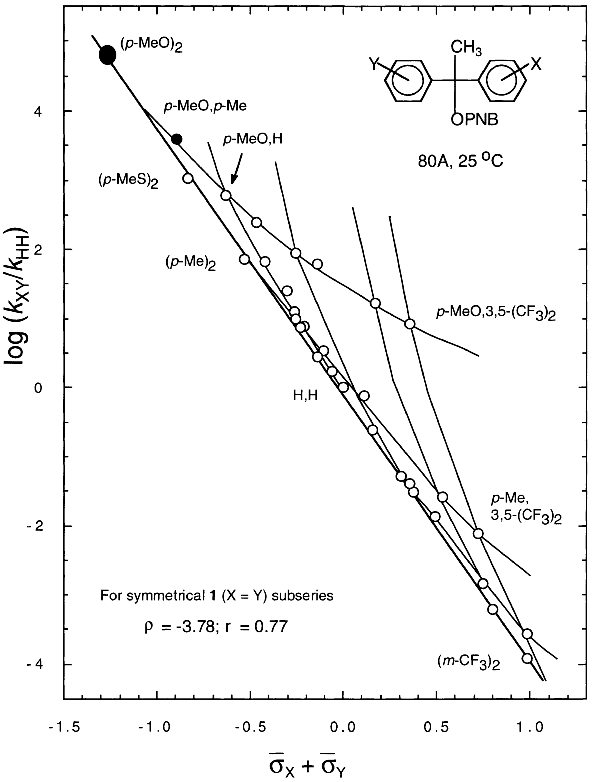

Fig. 2. Plots of log (k_{XY}/k_{HH}) for the solvolysis of 1,1-diphenylethyl *p*-nitrobenzoates against $\bar{\sigma}_X + \bar{\sigma}_Y$ with r_{sym} = 0.77.

fined by symmetrical subseries **1** at the point X = Y (Fig. 2). A nonlinear correlation analysis has been carried out for the respective Y-subsets using the More O'Ferrall equation (Eq. 4). The curved correlations for **2** (Y = H), **3** (Y = *p*-MeO), **4** (Y = *p*-Me), and when Y = *m*-Cl, were treated by Eq. 4 using the same $\bar{\sigma}_X$ scale (at r_{sym} = 0.77) as was used for the symmetrical subseries **1**. Similarly treated were the nonlinear correlations for other subsets, as summarized in Table 6.

In Table 6, the tangent $(\rho_o)_Y$ values change widely from subset to subset. They are roughly of the same magnitude, or to a good approximation proportional to the $(\rho_X)_Y$ values for the corresponding Y–T correlations in Table 5. Most important, both show the same dependence upon Y; the more electron-withdrawing Y is, the more negative the $(\rho_o)_Y$ value is. The $(2m)_Y$ coefficient remains constant at 0.5 for the subsets of different fixed-Y-substituent, indicating the same degree of curvature and the same shape of bent-back curvature for all subsets, as seen in Fig. 2.

The concave correlation line for these fixed-Y-subsets and the linear correlation for the symmetrical subseries touch at the point X = Y when the fixed-Y is in the middle of substituent range. In other cases, the correlation curve merges with the line of the symmetrical subseries' correlation at the point X = Y when Y is located at the ends of the substituent range studied. The tangent ρ value at the contact point X = Y of any Y subsets should be nearly the same as the ρ_{sym} value for the symmetrical subseries. Thus, provided that the zero-point (X = H) in the $\bar{\sigma}_X$ scale of any Y-subsets' correlation may be allowed to shift to the point of contact (X = Y), all the correlations for the Y-subsets should have an identical shape, with $(\rho_o)_Y = \rho_{sym}$.

Discussion

The correlation results in Table 5 indicate that the apparent $(\rho_X)_Y$ values of the Y–T correlations for Y-subsets with variable X-substituents change significantly with Y, in an approximate trend of a linear decrease of $(\rho_X)_Y$ as Y for the respective subsets becomes more electron-donating. The observed dependence of ρ_X values upon the fixed-Y-substituents appears to be in accord with the changes caused for an early transition-state expected from the *Hammond–Leffler rate-equilibrium relationship* (*or extended Brønsted relationship*).[12]

This elegant conclusion, however, relies heavily upon the validity of the Y–T correlations for the respective Y-subsets. While subsets **3** (Y = *p*-MeO) and **4** (Y = *p*-Me) gave Y–T correlations of *excellent* precision level, the apparent $(\rho_X)_Y$ values were based only on the electron-withdrawing range of substituents and their *r*-values which are based on a single *p*-MeO group are statistically indefinite. Analogously, for the electron-withdrawing Y-subsets, the correlation encompasses the electron-donating range, and there is no evidence that the same $(\rho_X)_Y$ value applies to the range of other substituents. It is noteworthy that analogous results were found for the bromination of 1,1-diarylethylenes.[3,13] The conclusion deduced above simply arises from the fact that the Y–T equation gives an excellent linear correlation for subset **2** (Fig. 3). The partial cor-

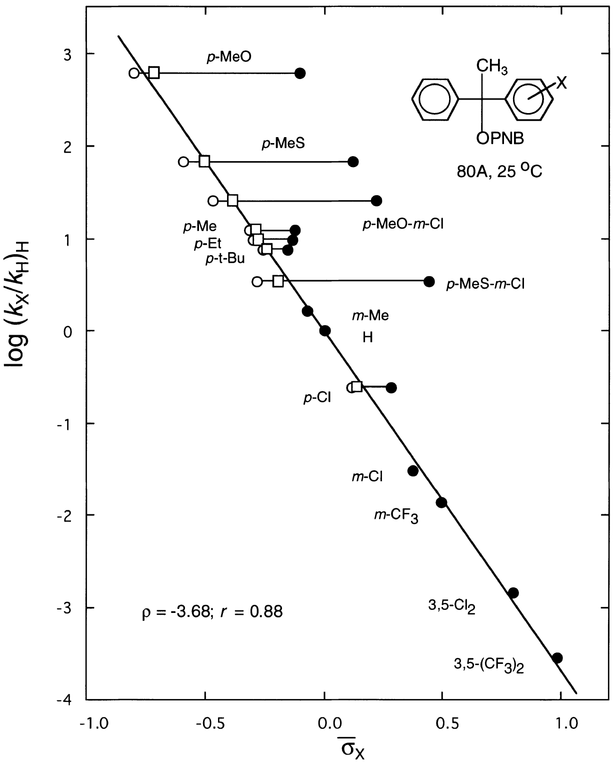

Fig. 3. Y–T plot for the solvolysis of monosubstituted 1,1-diphenylethyl *p*-nitrobenzoates **2** (Y = H): Closed circles for σ^{o}, open circles for σ^{+}, and open squares for $\bar{\sigma}$, respectively.

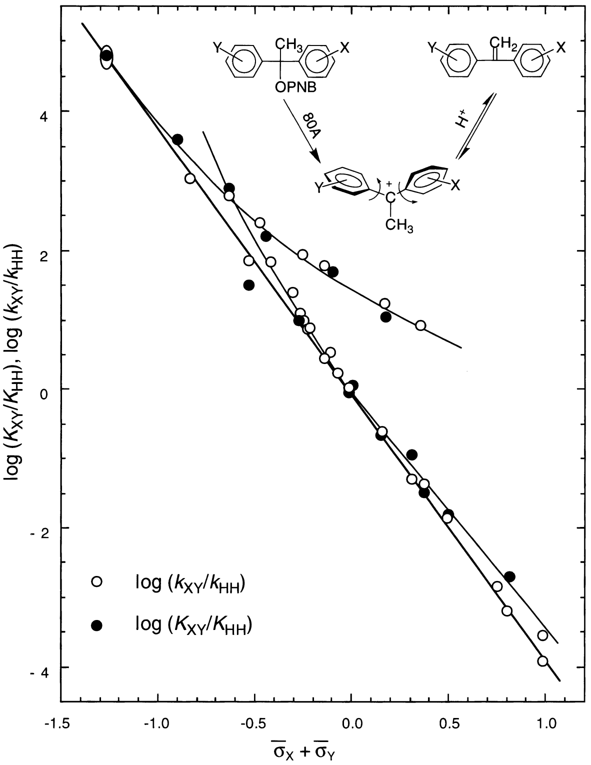

Fig. 4. Plots of log (k_{XY}/k_{HH}) for the solvolysis of 1,1-diphenylethyl *p*-nitrobenzoates and log (K_{XY}/K_{HH}) values against $\bar{\sigma}_X + \bar{\sigma}_Y$ with $r = 0.77$: Open circles for solvolyses and solid circles for equilibria.

relations for (a) strong π-donor substituents and for (b) electron-withdrawing substituents, are clearly different, indicating a non-linearity of the Y–T correlation for this subset.

It is therefore remarkable that the symmetrical subseries **1**(X = Y) gives an excellent linear correlation against $2\bar{\sigma}_X$ over the whole-range of substituents. However, the simple additivity relationship, Eq. 6, against $\bar{\sigma}_X + \bar{\sigma}_Y$ holds only for a severely limited range, but it gives a wide dispersion pattern as in Fig. 2 when $\bar{\sigma}_X$ differs significantly from $\bar{\sigma}_Y$ for the fixed-substituent Y. This characteristic dispersion pattern of the additivity relationship has been generally observed for multi-substituent effects in many typical α,α-diaryl carbocation forming processes,[3] such as the solvolysis of ArAr′C(CF_3)X system,[16–18] the ionization equilibria (pK_{R^+}) and nucleophile-recombination reactions of ArAr′Ar″C^+,[6] the hydrolysis and alcoholysis of the diarylmethyl systems,[4,5] and the hydration[9] and bromination[13] of ArAr′C=CH_2.[7,8]

From analogy with the behavior of closely related systems, a "concave plot," where both extreme ends of the plot are bent back upward from the reference line, is the best description of the shape of the correlation for the substituent-effect of the respective subsets. The individual correlation of any Y subset is concave and may be treated by the More O'Ferrall equation (Eq. 4). The tangent $(\rho_o)_Y$ value for the respective fixed Y-subset which has essentially the same physical meaning as the apparent $(\rho_X)_Y$ value in the Y–T correlation, varies similarly to the latter: It becomes more negative when Y becomes more electron-attracting. This variation can be referred to as a Hammond shift of the transition state, provided that it is due to the coordinate-shift of the transition state.[11,12]

The positive $(2m)_Y$ coefficient in Eq. 4 implies an assignment of a "concave plot" for any Y-subset: The shape of the plot should be related to the anti-Hammond shift of the transition state coordinate (or the late transition state) for rate-accelerating substrates. This conflicts with deductions from the behavior of other selectivity indices, especially with the so-called saturation effect that is expected from the More O'Ferrall theory.[5,10,11] This, in turn, leads to the conclusion that the signifi-

Table 6. Analysis of Substituent Effects by Eq. 4

No.	System	Y	$n^{a)}$	$(\rho_o)_Y$	$(2m)_Y$	R	SD
1		*m*-Cl	10	−5.03 ± 0.30	0.50 ± 0.68	0.9919	±0.21
2	**2**	H	14	−4.04 ± 0.05	0.51 ± 0.09	0.9994	±0.07
3	**4**	*p*-Me	6	−3.58 ± 0.13	0.40 ± 0.21	0.9988	±0.14
4	**3**	*p*-MeO	8	−2.58 ± 0.04	0.67 ± 0.06	0.9996	±0.04

a) Number of substituents involved.

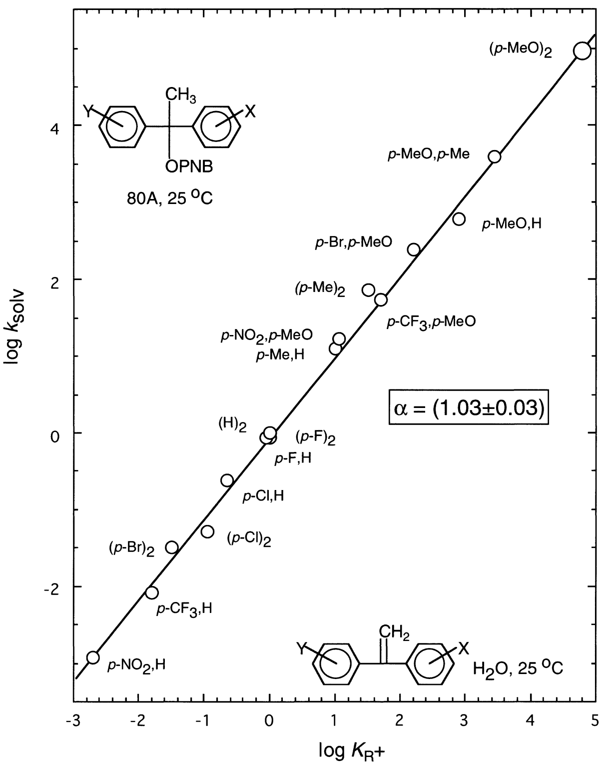

Fig. 5. A linear relationship between log k_{solv} for the solvolysis of 1,1-diphenylethyl *p*-nitrobenzoates and the corresponding log K_{R^+} values; log $(k_{XY}/k_{HH})_{OPNB} = -(1.03 \pm 0.03)\,\Delta pK_{R^+}$.

cant non-linearity observed in correlations of the Y-subsets does not arise from the coordinate-shift of transition state. As the More O'Ferrall coefficient $(2m)_Y$ remains approximately constant irrespective of the Y subset, the deviation from the linear correlation remains the same, implying no change in the position of the transition state.

This complicated *Substituent–Reactivity Relationship* is incompatible with the expectation from the RSR and the details are also incompatible with the conventional interpretation of a coordinate-shift of the transition state as a single effect.

The characteristic dispersion of this non-additivity relationship appears to be general in many α,α-diaryl carbenium ion-forming processes. Among them, highly relevant for the present study is the protonation equilibria of 1,1-diarylethylenes. Despite the extensive dispersion pattern with branches for respective Y-subsets of the correlations against $\bar{\sigma}_X + \bar{\sigma}_Y$, we have found that these plots of the literature pK_{R^+} values against $\bar{\sigma}_X + \bar{\sigma}_Y$ for 1,1-diarylethylenes, can be surprisingly precisely superimposed upon the non-additivity plot of the solvolysis of *p*-nitrobenzoates (OPNB) in Fig. 4. This finding is equivalent to a precise extended Brønsted relationship (7):[12]

$$\log (k_{XY}/k_{HH})_{OPNB} = -(1.03 \pm 0.03)\Delta pK_{R^+} \tag{7}$$

which is demonstrated in Fig. 5 as a linear relationship with a single slope between log $(k_{XY}/k_{HH})_{OPNB}$ for the solvolysis and ΔpK_{R^+} values. We hesitate to ascribe mechanistic significance to the derived value of Brønsted α coefficient of 1.03, since different solvents were used for the solvolysis and the equilibria measurements. We emphasize that, while any Y-subset shows a different dependence upon the X-substituents in either the solvolysis or the pK_{R^+}, they all satisfy the rate-equilibrium relationship (7) with a single α; i. e., both the susceptibility and the degree of curvature of the nonlinear correlation of any Y-subset are the same for the rates and the equilibria. Hence, the Brønsted relationship (8a),

$$\log (k/k_o)_Y = \alpha \log (K/K_o)_Y \tag{8}$$

should embrace any Y subsets, regardless of whether their Hammett-type correlations are linear or not. If a linear correlation holds for any individual Y-subset, Eq. 8a should also be satisfied with the same α-coefficient for the rate-equilibrium system of the subsets.

$$(\rho^k)_Y = \alpha(\rho^t)_Y \tag{8a}$$

Whatever the reason of the non-linearity and non-additivity behavior of any selectivity parameter, such as $(\rho^k)_Y$, $(2m)_Y$, and $(\rho_o)_Y$, the constant α coefficient serves as convincing evidence for the absence of a coordinate-shift of the transition state in this rate process. The changes in $(\rho^k)_Y$ with the subsets is independent of coordinate-shifts of the transition state in the rate process studied.

For the hydration of 1,1-diarylethylenes where the intermediate carbenium ion is identical with that for the present solvolysis, we expect a close pattern of the kinetic substituent effect, without the effect associated with coordinate-shifts of the transition state. The same expectation may be extended to the bromination of 1,1-diarylethylenes, for which a quite similar dispersion pattern to the additivity correlation in Fig. 2 was found, although the susceptibility parameters, e.g., $\rho_{sym} = -3.43$ and $r_{sym} = 0.56$ for the symmetrical olefins (X = Y), are slightly lower than those of the solvolysis. So far a great importance was attached only to the favorable dependence of the apparent ρ_X values on the fixed Y-substituents. Dubois and co-workers concluded therefrom[7] that the non-additivity in the bromination reaction arose not only from changes in the stability of the cationic intermediate but also from a significant coordinate-shift of the transition state, in contrast with our conclusion. Further comparative study of both reactions is required to clarify the major cause of this characteristic non-additivity pattern.

The characteristic dispersion pattern of the non-additivity relationship has been observed also for the α-CF_3-diarylmethyl system;[16–18] the observed variation of the selectivity ρ_X within any given Y-subset displayed a dependence of ρ_X upon the extent of deviation from the symmetrical propeller conformation of the aryl groups in the α,α-diaryl carbocations (or in the corresponding transition states). Thus the significant non-linearity and non-additivity observed in the α-CF_3 system were ascribed to a substituent-dependent conformational change rather than to a coordinate-shift of the transition state.

Although we presently prefer not to speculate on the reason for the significant non-linearity and non-additivity, the nonlinear Y–T correlations in the 1,1-diphenylethyl system may also result from a substituent-dependent varying conformation of

Table 7. Physical and Analytical Data of 1,1-Diarylethyl Alcohols and *p*-Nitrobenzoates

Substituents		Mp	Carbon/%		Hydrogen/%		Nitrogen/%	
X	Y	°C	Found	Calcd	Found	Calcd	Found	Calcd
Alcohol								
p-MeO	H	Liq.	78.40	78.92	7.11	7.06		
p-MeO-*m*-Cl	H	Liq.	68.49	68.57	5.93	5.75		
p-MeS	H	Decomp[a)]	73.66	73.73	6.61	6.60		
p-MeS	*p*-MeS	107–108	65.67	66.16	6.14	6.25		
p-Me	*p*-Me	Liq.	84.49	84.91	7.48	8.02		
p-Me	H	Liq.	84.63	84.87	7.57	7.60		
p-Et	H	Liq.	84.61	84.91	8.23	8.02		
p-*t*-Bu	H		84.95	84.99	8.65	8.72		
p-MeS-*m*-Cl	H	Liq.	64.65	64.62	5.33	5.42		
m-Me	*m*-Me	Liq.	84.50	84.91	7.94	8.02		
m-Me	H	Liq.	84.87	84.87	7.62	7.60		
H	H	81.0	84.73	84.81	7.10	7.12		
m-Cl	H	Liq.	72.39	72.26	5.65	5.63		
m-CF_3	H	Liq.	67.66	67.66	4.94	4.92		
p-Cl	H	Liq.	72.32	72.26	5.68	5.63		
p-Cl	*p*-Cl	Liq.	63.18	62.94	4.63	4.53		
3,5-Cl_2	H	Liq.	63.30	62.94	4.70	4.53		
3,5-$(CF_3)_2$	H	Liq.	57.52	57.49	3.70	3.62		
p-Me	*m*-Cl	Liq.	73.20	73.02	6.23	6.13		
	3,5-Cl_2	Liq.	64.38	64.07	5.18	5.02		
	3,5-$(CF_3)_2$	101	58.63	58.63	4.05	4.05		
p-MeO	*m*-Cl	Liq.	68.62	68.57	5.79	5.75		
	3,5-Cl_2	49	61.02	60.62	4.80	4.75		
p-Nitrobenzoates								
H	H	135.0decomp[b)]	72.53	72.61	4.97	4.93	4.03	4.03
p-Cl	H	115	66.01	66.06	4.33	4.22	3.62	3.67
m-Cl	H	118	64.80	66.06	4.19	4.22	4.05	3.67
m-CF_3	H	95	63.64	63.62	3.91	3.88	3.32	3.37
p-CF_3	H	122[c)]	63.72	63.62	3.90	3.88	3.47	3.37

a) Decomp at temp above 35 °C. b) Lit.[19] mp 135 °C decomp. c) Lit.[19] mp 121.5–122 °C.

the transition state. In order to investigate this effect on the selectivity parameters ρ_X and r on the fixed-substituents Y, we have extended our investigations to widely varying Y substituent systems. This will be reported in the following papers.

Experimental

All melting points are uncorrected. ^{1}H NMR spectra in $CDCl_3$ were recorded on a JEOL JNM-A500 FT-NMR spectrometer operating at 500 MHz and the chemical shifts are given in ppm (δ) downfield from TMS as an internal standard. The NMR data were deposited as Document No. 75031 at the Office of the Editor of Bull. Chem. Soc. Jpn.

Materials. Monosubstituted 1,1-diphenylethyl alcohols were prepared by the reaction of acetophenones with appropriate Grignard reagents in dry ether. Symmetrically disubstituted alcohols were prepared by treating ethyl acetate with the Grignard reagents. 1,1-Diphenylethyl *p*-nitrobenzoates were prepared from the lithium alkoxide and *p*-nitrobenzoyl chloride in tetrahydrofuran according to the general procedure reported by Brown and Peters.[21] The chlorides were prepared by reacting the alcohols with $SOCl_2$ in dry benzene at 0 °C.[16a,17] The physical properties of the tertiary alcohols and *p*-nitrobenzoates are summarized in Table 7.

1,1-Bis(*p*-methylphenyl)ethyl Alcohol. To magnesium turnings (1.74 g, 71.5 mmol) under nitrogen atmosphere, *p*-bromotoluene (11.12 g, 65.0 mmol) in 30 mL dry ether was added dropwise at room temperature, and the mixture was stirred for 3 h. A solution of ethyl acetate (2.64 g, 30 mmol) in 30 mL dry ether was slowly added to the Grignard reagent solution and the mixture was stirred for an additional 3 h at room temperature. To the ice-bath cooled reaction mixture, aqueous NH_4Cl (3.38 g, 63.2 mmol) was added dropwise over 20 min and then the mixture was extracted with ether. The extract was washed with aq NaCl solution and dried over anhydrous $MgSO_4$. After evaporation of the solvent, the residue (5.90 g) was flash chromatographed on silica gel 60 (230–400 mesh, Merck) to give the alcohol as a colorless liquid (1.84 g, 26% yield). Other bis-substituted alcohols were synthesized similarly.

1-(*m*-Chloro-*p*-methoxyphenyl)-1-phenylethyl Alcohol. A solution of acetophenone (3.60 g, 30 mmol) in 30 mL dry ether which was slowly added to the solution of a Grignard reagent prepared from magnesium (0.87 g, 35.75 mmol) and *o*-chloro-*p*-bromoanisole (7.20 g, 32.5 mmol) in 30 mL dry ether was stirred for 3 h at room temperature. The mixture was then quenched by aq NH_4Cl (1.69 g, 31.6 mmol) at ice bath temperature and extracted with ether. The combined organic layer was washed with aq NaCl solution, dried over anhydrous $MgSO_4$, and evaporated under reduced pressure. The residue (7.41 g) was flash chromatographed on silica gel to give the alcohol as a colorless liquid (5.37 g, 75% yield). Other unsymmetrically substituted alcohols were synthesized similarly from the appropriate acetophenones and the Grignard reagent.

1,1-Bis(*p*-methylthiophenyl)ethyl *p*-Nitrobenzoate. To the corresponding alcohol (1.45 g, 5 mmol) in 5 mL of THF, 15% butyllithium in hexane (5 mL, 7.5 mmol) was added dropwise at 0 °C under nitrogen and then the mixture was stirred for 3 h. A solution of *p*-nitrobenzoyl chloride (0.93 g, 5 mmol) in 5 mL THF was added slowly to the mixture at −30 °C, the mixture was stirred for 30 min, and then allowed to warm to room temperature with stirring for an additional 3 h. The reaction mixture was quenched by slowly adding ice-cooled water (13 mL) and extracted with ether. The ether extract was washed with ice-cold 5% aq $NaHCO_3$, and then with aq NaCl solution, dried over anhydrous $MgSO_4$, and kept in solution in dry ether. Since the *p*-nitrobenzoates were unstable and formed olefins, they were used directly for kinetic measurements immediately after evaporation of the solvent. Other esters were synthesized similarly.

1,1-Bis[*m*(trifluoromethyl)phenyl]ethyl Chloride. To the corresponding alcohol (0.83 g, 2.5 mmol) in 4 mL of dry benzene containing dry pyridine (0.20 g, 2.5 mmol), $SOCl_2$ (5.95 g, 50 mmol) was added dropwise at 0 °C and the reaction mixture was stirred for 30 min. The solvent was evaporated under reduced pressure and the residue was dissolved in dry benzene. The precipitated pyridinium salt was filtered, and the solvent was evaporated under reduced pressure. The same procedure was repeated by adding new dry benzene in order to remove completely the excess $SOCl_2$ and salts. Since the chlorides were very unstable and formed an appreciable amount of olefins, they were used directly for kinetic measurements immediately after evaporation of the solvent. Other chlorides were prepared similarly from the corresponding alcohol.

Solvents. Commercial acetone was refluxed with $KMnO_4$ for 6 h and distilled. The distillate was dried over anhydrous Na_2CO_3 and redistilled. HPLC grade distilled water (Chameleon reagent) was distilled immediately before use. 80% (v/v) and 50% (v/v) aqueous acetone mixtures for the solvolysis studies were prepared by mixing the corresponding volumes of acetone and water at 25 °C.

Kinetic Measurements. The solvolysis rates were determined conductimetrically as reported previously[17] at initial concentrations of ca. 10^{-5} for *p*-nitrobenzoates and 10^{-4} mol dm^{-3} for chlorides. CM-60S and CM-50AT (Toa Electronics Ltd.) conductivity meters were equipped with an interval time unit and printer and those of CM-60V, CM-40G, and CM-40V were connected to a high speed personal computer. Solvolysis was followed in a thermostatted bath controlled within ±0.01 °C by taking at least 100 readings at appropriate intervals during 2.5 half-lives, and an infinity reading after 10 half-lives. The experimental errors in the respective runs were generally less than 1.0% and reproducibility of the rate constants was within ±1.5%. The first-order rate plots were satisfactorily linear over 2.5 half-lives with a correlation coefficient > 0.99997.

References

1 a) Y. Yukawa and Y. Tsuno, *Bull. Chem. Soc. Jpn.*, **32**, 971 (1959). b) Y. Yukawa, Y. Tsuno, and M. Sawada, *Bull. Chem. Soc. Jpn.*, **39**, 2274 (1966).

2 Y. Tsuno and M. Fujio, *Chem. Soc. Rev.*, **25**, 129 (1996).

3 Y. Tsuno and M. Fujio, *Adv. Phys. Org. Chem.*, **32**, 267 (1999).

4 a) S. Nishida, *J. Org. Chem.*, **32**, 2692, 2695, 2697 (1967). b) J. R. Fox and G. Kohnstam, *Proc. Chem. Soc.*, **1964**, 115. c) M. Fujio et al., unpublished result.

5 J. Mindle and M. Vecera, *Collect. Czech. Chem. Commun.*, **37**, 1143 (1972). J. Mindle and M. Vecera, *Collect. Czech. Chem. Commun.*, **36**, 3621 (1971).

6 N. C. Deno and A. Schriesheim, *J. Am. Chem. Soc.*, **77**, 3051 (1955). N. C. Deno and W. L. Evans, *J. Am. Chem. Soc.*, **79**, 5804 (1957). C. D. Ritchie, *Can. J. Chem.*, **64**, 2239 (1986). R. A. McClelland, V. M. Kanagasabapathy, N. S. Banait, and S. Steenken, *J. Am. Chem. Soc.*, **111**, 3966 (1989). R. A. McClelland, V. M. Kanagasabapathy, N. S. Banait, and S. Steenken, *J. Am. Chem. Soc.*, **113**, 1009 (1991).

7 M. F. Ruasse, *Adv. Phys. Org. Chem.*, **28**, 207 (1993).

8 a) J. E. Dubois, M. F. Ruasse, and A. Argile, *J. Am. Chem. Soc.*, **106**, 4840 (1984). b) M. F. Ruasse, A. Argile, and J. E. Dubois, *J. Am. Chem. Soc.*, **106**, 4846 (1984).

9 G. Goethals, F. Membrey, B. Ancian, and J. P. Doucet, *J. Org. Chem.*, **43**, 4944 (1978).

10 M. O'Brien and R. A. More O'Ferrall, *J. Chem. Soc., Perkin Trans. 2*, **1978**, 1045.

11 D. J. McLennan, *Tetrahedron*, **34**, 2331 (1987).

12 a) G. S. Hammond, *J. Am. Chem. Soc.*, **77**, 334 (1955). b) J. E. Leffler and E. Grunwald, "Rates and Equilibria of Organic Reactions," Wiley, New York (1963). c) E. S. Lewis, C. C. Shen, and R. A. More O' Ferrall, *J. Chem. Soc., Perkin Trans. 2*, **1981**, 1084.

13 J. E. Dubois, A. F. Hegarty, and E. D. Bergmann, *J. Org. Chem.*, **37**, 2218 (1972). A. F. Hegarty, J. S. Lomas, W. V. Wright, E. D. Bergmann, and J. E. Dubois, *J. Org. Chem.*, **37**, 2222 (1972).

14 C. D. Johnson, *Tetrahedron*, **36**, 3461 (1980). B. Giese, *Angew. Chem., Int. Ed. Engl.*, **16**, 125 (1977).

15 R. A. Marcus, *J. Phys. Chem.*, **72**, 891 (1968). J. R. Murdoch, *J. Am. Chem. Soc.*, **94**, 4410 (1972). G. W. Koppel and A. J. Kresge, *J. Chem. Soc., Chem. Commun.*, **1973**, 371.

16 a) M. Fujio, H. Morimoto, H.-J. Kim, and Y. Tsuno, *Bull. Chem. Soc. Jpn.*, **70**, 1403 (1997). b) M. Fujio, H. Morimoto, H.-J. Kim, and Y. Tsuno, *Bull. Chem. Soc. Jpn.*, **70**, 3081 (1997).

17 M. Fujio, H.-J. Kim, H. Morimoto, S.-D. Yoh, and Y. Tsuno, *J. Phys. Org. Chem.*, **12**, 843 (1999).

18 M. Fujio et al., to be published in *J. Phys. Org. Chem.*

19 H. C. Brown, M. Ravindranathan, and E. N. Peters, *J. Org. Chem.*, **42**, 1073 (1977).

20 M. K. Uddin, M. Fujio, and Y. Tsuno, to be published in *J. Phys. Org. Chem.*

21 H. C. Brown and E. N. Peters, *J. Am. Chem. Soc.*, **97**, 1927 (1975).